

DESIGN AND CFD ANALYSIS OF A NEW ROTARY GAS COMPRESSOR

²Dimitrios Vogiatzis*, ¹Evangelos Mallios, ¹Savvas Savvakis, ²Zissis Samaras

¹theSARMproject, Greece

²Laboratory of Applied Thermodynamics, Aristotle University of Thessaloniki, Greece

KEYWORDS –

theSARMproject, gas-compressor, oil free, air-compressor, compressor, SARM, CFD, ANSA, CONVERGE, META

ABSTRACT –

Amid the increasing demand for higher compression levels in gas compressors, the innovative design of a novel rotary thermal engine, called SARM, favours the development of a new configuration of gas compressors. This study aims to use Computational Fluid Dynamics (CFD) simulations to develop the models of three different applications and compare the existing gas-compressors with the one inspired by the SARM engine. For the high-transient simulations, this study uses the pre-processing software ANSA in conjunction with the CONVERGE CFD solver, and the post-processing software META. With an even higher power-to-weight ratio of today's most high-tech compressors, oil-free sealing method, significantly lower number of components and calculated peak pressure of 27 bar in the best-case scenario, the presented type of gas compressors can be the game changer in a range of different applications.

TECHNICAL PAPER –

1. INTRODUCTION

Compressed gas accounts for an approximately 10% of the global industrial electric energy consumptions [1] and this share may reach up to 20%, including commercial and residential needs (such as portable tools, air pumps, pneumatic heating, ventilation, air conditioning) [2]. In order to reduce energy consumption, energy saving is a crucial factor for the gas compression industry in parallel with the continuously increasing demand for compressed gas, worldwide. Upstream and downstream of the gas compressor are actions that focus on energy savings, such as pipeline leakage reduction, reduction of frictional losses, optimisation of the end user devices. However, the future saving potentials are estimated to be no higher than 15% [3] for the established maximum power and power-to-weight ratio.

Positive displacement gas compressors work by filling a chamber with gas and then reducing the chamber's volume. What characterises this type of compressors is the higher Compression Ratio (CR) and lower mass flow in comparison with the dynamic compressors, such as turbo-compressors with an axial or radial flow pattern [4].

The four main categories of positive displacement gas compressors that today are the most widespread and efficient in the industry field are the following:

- the reciprocating piston compressor (RecipC),
- the rotary screw compressor (ScrewC),
- the rotary scroll compressor (ScrollC) and
- the rotary vane compressor (Sliding Vane rotary compressors or SVRC).

As for the reciprocating piston compressor, the single stage can reach up to 12 bar maximum output pressure in the largest size [5], and, in general, they have a wide range of applications. They are simple and reliable, but they are dealing with sealing, noise and vibration problems when designed on high CR. On the other hand, the Rotary screw compressor can reach a maximum output pressure of 12 bar in oil-free design [6] and 20 bar when they use oil lubrication [4], but this is only for heavy stationary

applications. Furthermore, the rotary scroll compressor is ideal for small and medium-size applications with a maximum pressure of 13 bar, mostly in lubricant conditions [7]. Last, the rotary vane compressor has a maximum pressure of 3 bar when it is oil-free and the best design of 12 bar when the oil is injected in the compression chamber [8].

On the other hand, this paper introduces and analyses the potential of a novel oil-free rotary compressor called SARC that has a design with higher power and efficiency and a much smaller weight and volume. The idea of this compressor is based on a new concept rotary internal combustion engine with an international patent in 13 countries [9].

In general, significant concern about the compressors' technology is the maximum developed pressure inside the compression chamber at the end of the compression process [10, 11]. This paper presents the CFD simulations and the followed optimisation procedure for the prototype compressor to investigate the maximum output pressure and general behaviour of the fluid inside the compressor. The design is made with very strict and defined constructional constraints because the purpose of this study is to lead the first experimental prototype of the compressor.

This novel design is applied in three scales for three different applications with the target to compare it with today's best single-stage compressors on every scale. The chosen application are the following:

- A portable small size application [40-50 m³/h]
- A portable medium size application [200-250 m³/h]
- An industry stationary big size application [1200-1300 m³/h]

2. TECHNICAL DESCRIPTION

Description of the SARC operating principle

The studied compressor was inspired by a new concept rotary engine called SARM. The compressor is essentially the intake & the compression chamber of the SARM engine and the operation principle of this engine is described below with the help of **Figure 1**:

- ✓ The piston (1) rotates with a speed of 3,000 to 12,000 rpm inside a concentric toroidal chamber (2).
- ✓ The piston (1) and the sliding port (SP) (3) divide the toroidal chamber (2) into two chambers; the intake chamber (4 α) and the compression chamber (4 β).
- ✓ The back side of the piston (1) drags atmospheric air through the intake-port (5) into the intake-chamber (4 α), while the front side of the piston compresses the trapped air between the piston and the SP inside the compression chamber (4 β).
- ✓ The SP (3) remains closed during the whole compression process. When the piston reaches the closed SP, the latter opens letting the piston to pass and then closes again.
- ✓ Valves (6 α & 6 β) open 10 degrees before the SP opening and the compressed air is delivered into the combustion chamber (7) through the pressure chamber (8).
- ✓ Injection process follows and then ignition and combustion process.

Figure 1 gives only the necessary parts of the real prototype in order to keep the description simple and understandable.

For a better understanding of the operation's principle, the reader may refer to the online video that describes the engine's operating principle [12].

Thermodynamic analysis

The thermodynamic principle is based on an isentropic compression. For the isentropic compression between start (1) and end (2) position of the piston the total energy added to the fluid by the shaft is:

$$q_{1-2} = 0 \Rightarrow \Delta u_{1-2} = w_{1-2} = c_v * (T_2 - T_1)$$

From the isentropic theory [13], we can calculate the maximum isentropic pressure and temperature of the compression.

$$P_2 = P_1 * CR^\gamma, \text{ when } CR = \frac{V_1}{V_2} \text{ and } T_2 = T_1 * \left(\frac{P_2}{P_1}\right)^{\frac{\gamma-1}{\gamma}}$$

The isentropic compression efficiency of SARC is calculated by comparing the ΔP of SARC with the ΔP of the isentropic process. So, it is defined by the following ratio:

$$\eta_{compressor} = \frac{h_2 - h_1}{h_{2,is} - h_1} = \frac{\int_1^2 T ds + v(P_2 - P_1)}{\int_1^{2s} T ds + v(P_{2,is} - P_1)} = \frac{P_2 - P_1}{P_{2,is} - P_1}$$

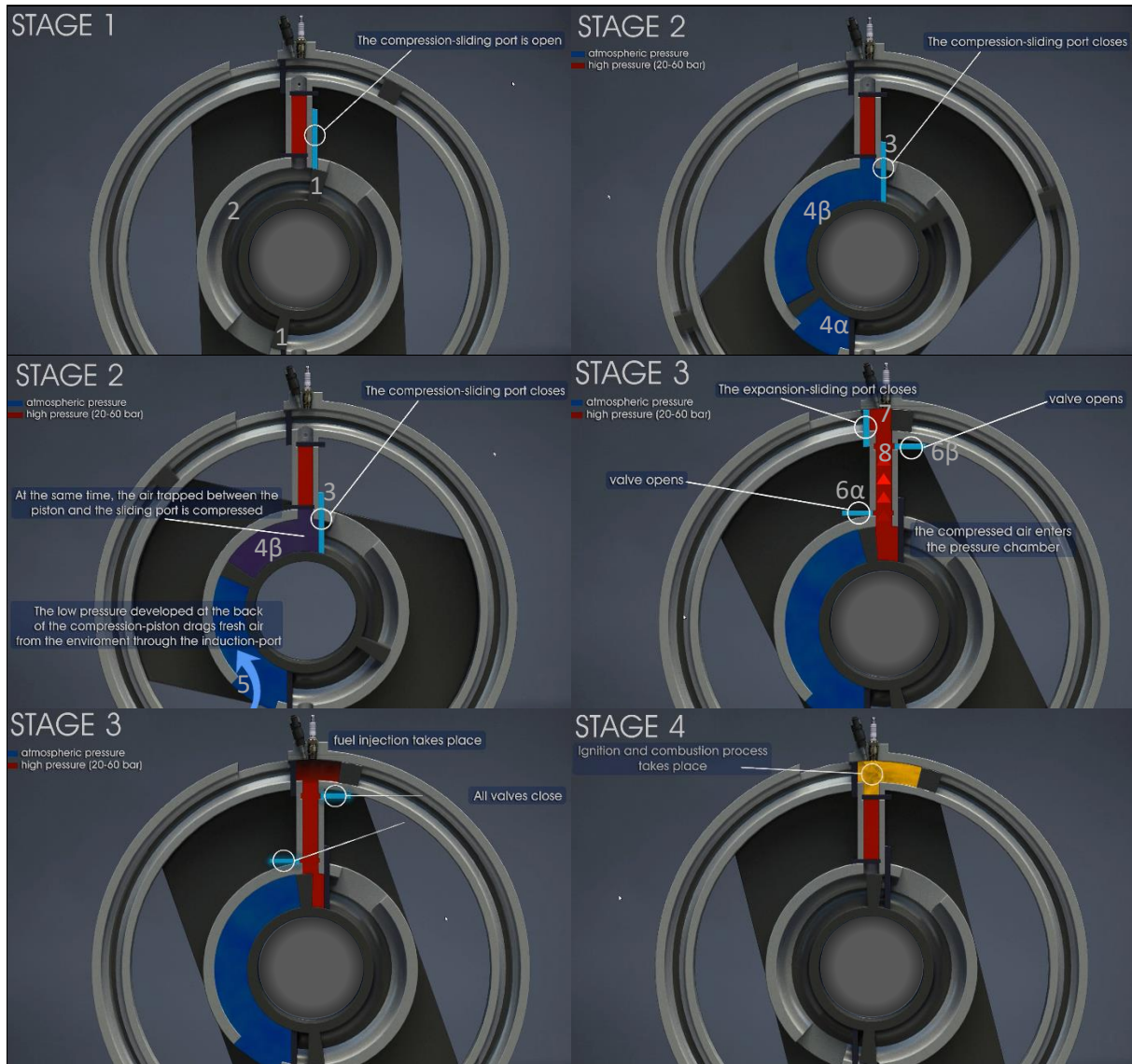


Figure 1 – Operating principle of the compressor

Advantages

The advantages of SARC are the following:

- ✓ Lack of lubricant inside the compression chamber.
- ✓ The applied forces are only in the direction of the flow allowing to the piston's sleeve to be very short.
- ✓ There are no mechanical losses and inertial forces from the conversion of reciprocating to rotational motion.
- ✓ The compressor's design is very simple, consisting of only a few parts allowing the compressor to be lighter and smaller than any other commercial compressor.

3. SIMULATION PROCESS

3D CAD design (SolidWorks)

The design has been created in SolidWorks for three different applications; small- medium- and big-size applications. **Figure 2** shows the magnitude of every scale, accordingly. Even though the basic idea is the compression chamber to be as close as possible to the compressor's shaft, the sealing system limits the minimum rotation radius.

The bigger the size of the application, the higher the torque required by the compression process because of the bigger shaft's diameter and the longer sealing system. The latter becomes longer to avoid the high pressure to leak to the environment gets longer.

On the other hand, the bigger the application, the higher the output pressure because the compression ratio can get higher.

The total weight and volume of each compressor are calculated in SolidWorks for the real design models and materials. For the small-size and medium-size applications, the overall weight and volume are crucial because they may also be portable. In the case of the big-size compressors, the weight is not so important because they are always stationary.

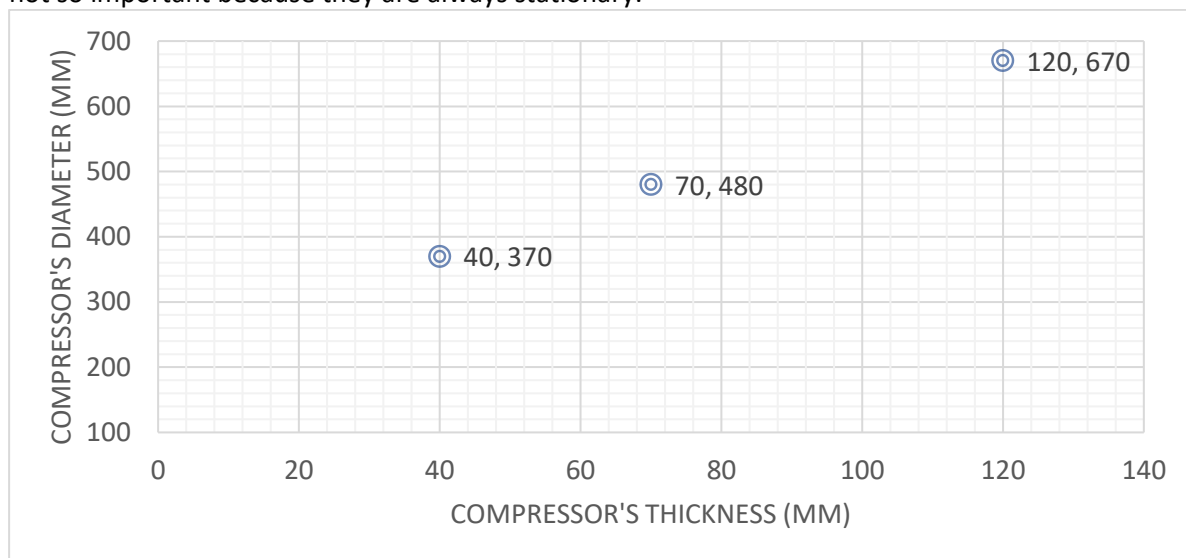


Figure 2 – The three different size applications

Pre-Processing (ANSA)

After defining the fluid-volume geometry inside SolidWorks, the model is inserted directly from SolidWorks to ANSA. The Boundary Conditions were automatically recognised with the help of the ANSA translation tool that can translate specific colours to specific PIDs.

After importing the model in ANSA, the Topology handling of ANSA offers an easy and fast preparation of the final watertight model. Before exporting the STL file for the solver, the minimum number of nodes is essential to keep the final file as small as possible.

The used CFD-solver "CONVERGE CFD" creates both the surface and volume mesh automatically. There is no need for the user to create a detailed, high-quality mesh. The only requirement is to input in the solver an STL file with the Geometry. However, the crucial part of this STL mesh is to depict in the highest quality all the details of the geometry. A very-fine STL mesh avoids intersections of the parts, especially when there are many curvatures in the geometry. On the other hand, a very fine mesh in regions where there are only flat surfaces can make the STL file heavy with no reason.

The Meshing tools of ANSA allow the automatic creation of an STL mesh with least possible nodes in flat surfaces and a controllable number of nodes in the curved edges. The last control is to create an ortho-triangle mesh in all curved surfaces. The whole methodology is made automatically with no additional time from the user.

Solver

CONVERGE CFD is the used solver for the CFD simulations.

CONVERGE CFD is mainly designed for simulations in internal flows and thermal engines of any nature, such as reciprocating or rotary internal combustion engines, turbomachines, pumps and compressors, boilers and burners. It is ideal for highly transient simulations with a variable mesh. Its revolutionary difference with other CFD solvers in the market is in the automatic creation of the grid. Thus, CONVERGE CFD creates a perfect rectangular structured grid based on simple user-defined parameters, without the need for the careful and time-consuming construction of the grid by the user [14]. Moreover, the user can use a rotation angle instead of time, which is ideal for rotational devices like this compressor.

The used turbulence model for this compressible flow is k-e RNG. Although the RSM model is ideal for simulating flows with intense vortices, pressure waves, high turbulence and direction's changes (such as curved pipes, cyclones), a compromise was necessary between the simulation time and accuracy of results due to the high computational cost. The k-e RNG model is widespread in 4-stroke Internal Combustion Engines (ICE), and after a benchmark between the two turbulence models, the results showed that there is a small difference in the solution but with an exceptionally longer simulation-time for the RSM [21].

Post-Processing (META)

The post-processing analysis and the visualization of the flow used the post-processor META. META offers a high-quality display of the flow field with the rendering tool in pictures and videos of the compressor in a quick and user-friendly environment. A script from technical support made possible the creation of an animation of the streamlines development for a complete operating cycle of the compressor (360 degrees), even though this was very difficult with any other post-processor because the script had to avoid the rotational force applied on the fluid for each time-step in order to give a correct visual result.

4. MODEL OPTIMIZATION METHOD

A CFD simulation should be as accurate as possible, and an accurate solution should be independent of the chosen time-step or Grid density.

Moreover, CONVERGE CFD recommends in the case of ICEs to run at least 5 to 30 operating cycles [14] in order to get a solution that is not affected by the operating cycles. Therefore, before running any case, the priority was to define the time-step, Grid-density and number of operating cycles for each case.

Time-independent study

As far as the time-step is concerned, CONVERGE CFD solver can ensure a time-independent study by using a variable time-step. Thus, by choosing a minimum of 10^{-8} and a maximum of 10^{-3} s time-step, for 3,000 rpm, the solver uses the optimum value according to the moving mesh's velocity and pressure rate of change.

Grid-independent study

Table 1 summarizes the comparison of peak pressure for three grid-densities for the small-size application. A grid of 400K could give a result that differs only 1.8% from the finest grid, so for the fastest simulation, all small-size Grids are based on this cell size. The two other applications followed the same procedure, and Table 2 gives the final grid size for every model.

Table 1 – Grid independent study results for Small SS.OI

	Number of Cells	peak Pressure	for each cycle
<i>Coarse Small.SS.II</i>	400K	16.9 bar	2 days
<i>Fine Small.SS.II</i>	650K	17.2 bar (+1.8%)	3 days
<i>Extra Fine Small.SS.II</i>	1.1M	16.6 bar (-1.8%)	5 days

Table 2 – Final Grid size for the three application models

	Based-Grid Cell-size	Number of cells
<i>Small</i>	1mm	400K
<i>Medium</i>	1mm	1.9M
<i>Big</i>	1mm	9M

“Operating Cycle”-independent study

According to Converge, the minimum number of complete operating cycles for an ICE to come in a steady state condition is 5 to 30 cycles. Thus, after choosing the right time-step and grid-size, the models run for five cycles for each application-size and the difference in the maximum developed pressure and temperature was fallen under 1% between the last two sequential cycles. Therefore, there was no need to run more than five cycles for each case. **Figure 3** shows the case of a big-size application.

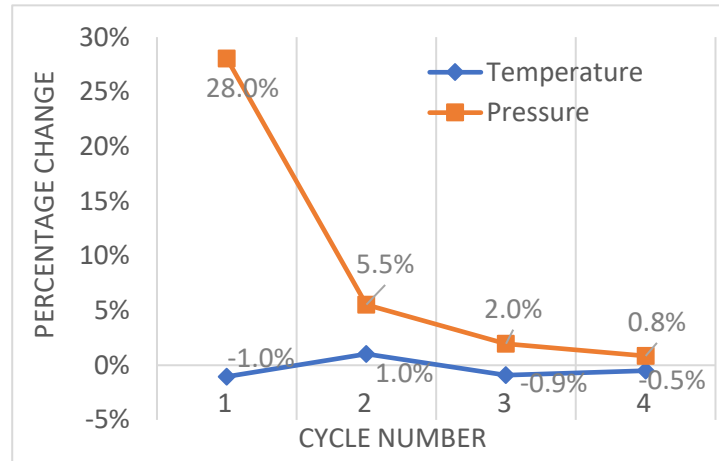


Figure 3 – Convergence of big size model

Optimisation study

The optimization procedure is based on two intake-port systems and two different lengths of the same sealing system. The two intake-port systems differ in shape. The first one is a rectangle shape intake-port and the second one is a geometry with optimized breathing for this specific toroidal chamber. The two intake configurations are recognized with II (Initial Intake) and OI (Optimized Intake) and the two different lengths of the sealing system with LS (Long Sealing) and SS (Short Sealing) due to their main difference in the characteristic sealing length.

Table 3 presents the calculated peak pressure and temperature by CFD, and the one calculated with the isentropic process equation. The name of every model is declared firstly with the application type, then the sealing technology and finally follows the intake-port system — for instance, Small.LS.II means “small-size application” – “Long Sealing System” – “Initial Intake-port”.

Table 3 – Results of the optimisation process in every application

Model	peak Pressure (bar) - CFD	peak Temperature (K) - CFD	peak Isentropic Pressure (bar)	peak Isentr. Temperature (K)	Isentropic efficiency of the compressor
Small.LS.II	14.1	581.4	26.3	764	53.6 %
Small.SS.II	15.9	588	26.3	764	60.6 %
Small.SS.OI	16.9	589.6	26.3	764	64.2 %
Medium.LS.II	17.0	574	28.7	783	59.2 %
Medium.SS.II	17.9	582.3	28.7	783	62.5 %
Medium.SS.OI	20.25	594	28.7	783	70.1 %
Big.LS.II	23.3	587	28.9	775	80.6 %
Big.SS.II	25.6	617	28.9	775	88.6 %
Big.SS.OI	26.9	614	28.9	775	93.1 %

For each application-size, Table 3 compares the short and long sealing system, and the best sealing length is then simulated with the optimized intake-port.

Like shown in **Figure 4**, in the case of the big-size application, the combination of the optimized intake-port and the long sealing-system manages to reach 13.2% higher peak-pressure compared to the baseline model.

In the case of the medium-size application, the improvement is 12.5% and in the case of the small-size application 10.6%.

Figure 5 compares all applications with the isentropic process, and the conclusion is that the bigger the size of the application, the higher the isentropic efficiency of the compressor.

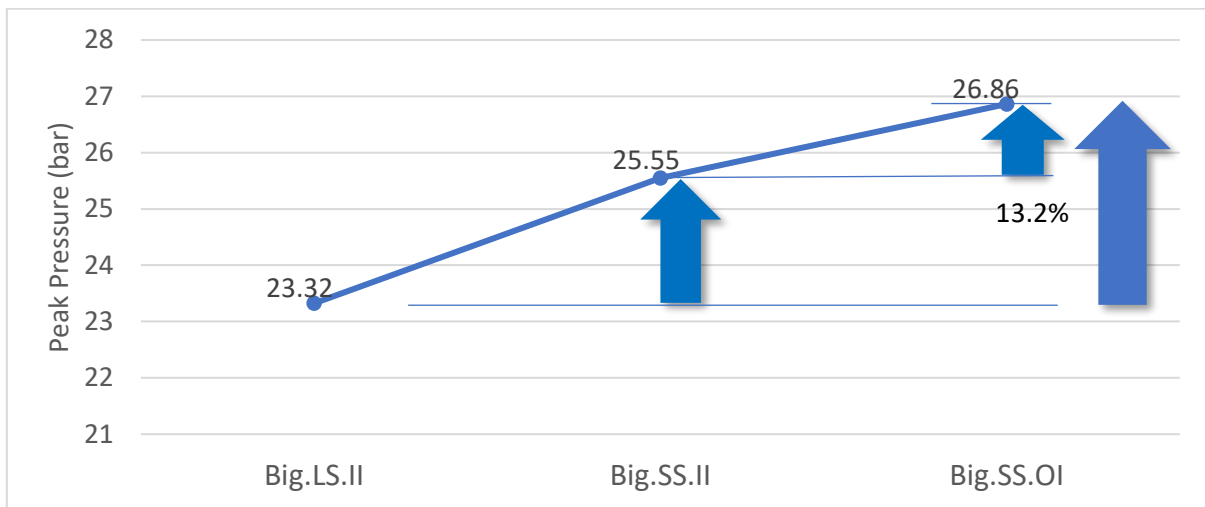


Figure 4 – Optimization of the big app model

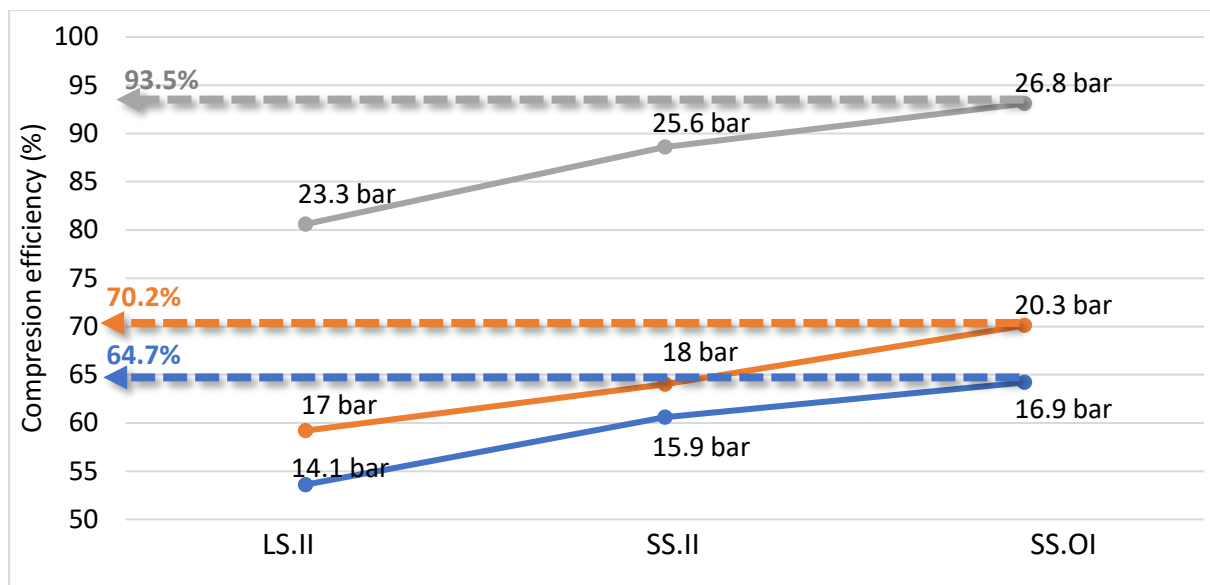


Figure 5 – Comparison of the optimisation study for the three applications

For the big-size application, in both sealing lengths and intake-port systems, the pressure development inside the compression-chamber is the same (

Figure 6).

On the other hand, in the intake-chamber, the optimized intake-port geometry gives 0.1 bar higher pressure along the whole operating cycle, compared to the initial intake-port (

Figure 7). This 0.1 bar ensures a better filling of the intake chamber with atmospheric air, and it leads to a higher peak pressure at the end of the compression process.

In the case of the small-size application, the increase is only 0.02 bar and in the case of medium-size application 0.01bar.

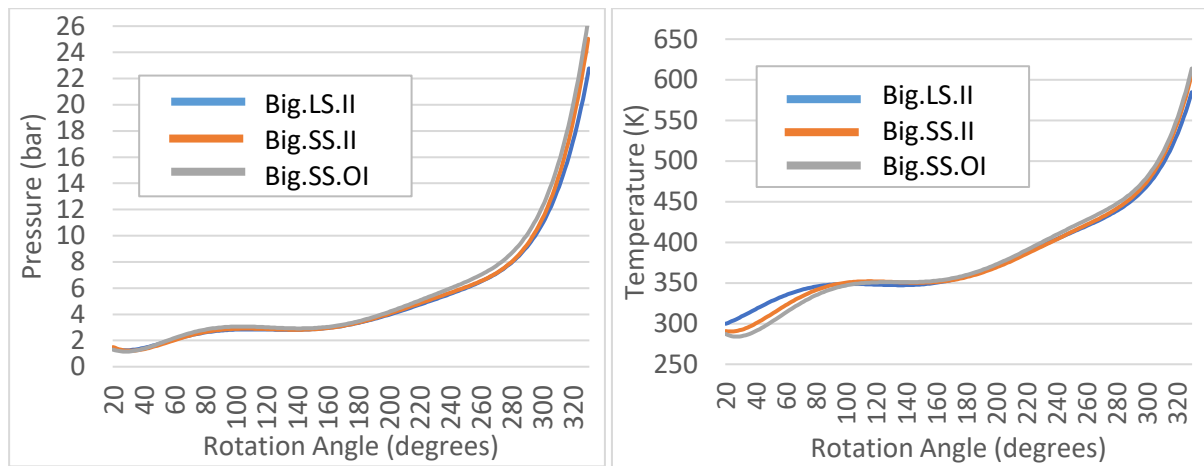


Figure 6 (a), (b) – Pressure and Temperature diagrams in the compression chamber

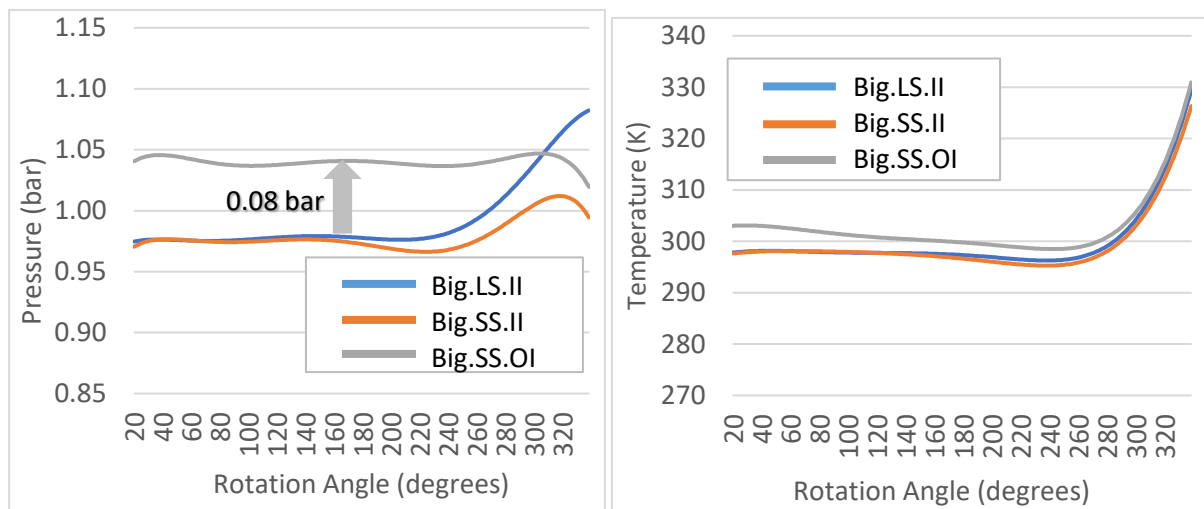


Figure 7 (a), (b) – Pressure and Temperature diagrams in the intake chamber

5. VISUALIZATION OF THE RESULTS

The post-processing in META showed that in all size applications, the fast closing of the SP develops a pressure wave that travels along the compression-chamber, hits on the SP and then comes back to the piston. This wave makes a reciprocating motion by hitting continuously on the piston and the SP. This wave comes from the very fast closing of the SP. The air trapped between the piston and the SP has a strong inertia and suddenly meets a closed wall at its front. This wall concentrates a significant amount of air that applies a strong force on the wall. On the other hand, the wall applies the same force on the concentrated air and eventually the air changes direction and it travels against the piston. This phenomenon is very strong at the start of the compression phase and it comes weaker during the development of the compression process.

6. COMPARISON OF THE THREE DIFFERENT SIZE-APPLICATIONS

The small-size type has to be portable. Thus, the volume and weight of each compressor are of most importance along with the energy consumption and the output pressure.

The medium-size compressors can be either portable or stationary, so the comparison is focused on the best stationary and portable compressors of this size.

Last but not least, the big-size compressors are all stationary, and the comparison in weight and volume between different types is less important than the comparison between energy consumption and the peak pressure.

Small size comparison

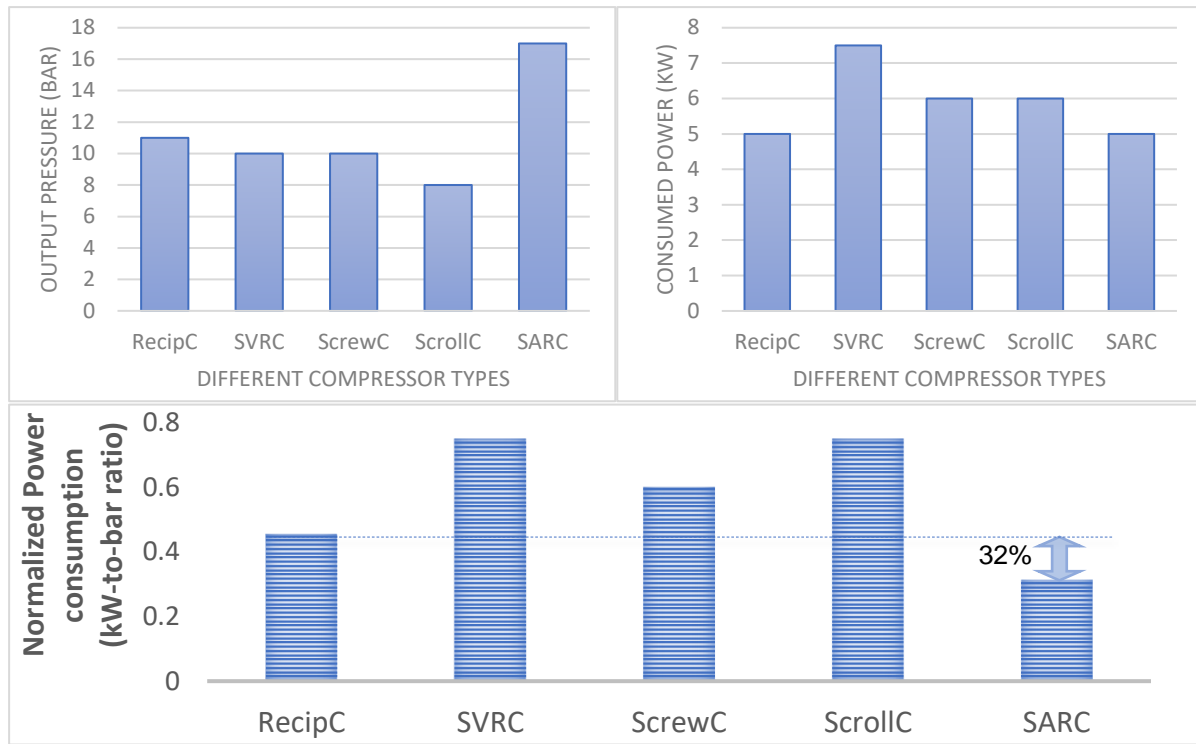


Figure 8 – Comparison of different types for small size applications

Medium size comparison



Figure 9 – Comparison of different types for medium size applications

Figures 9-11 compare this type of compressor with the competing technologies in terms of maximum pressure (a), consumed power (b) and the normalized power consumption (c). The latter term shows how many kW requires each 1bar of compression.

Big size comparison

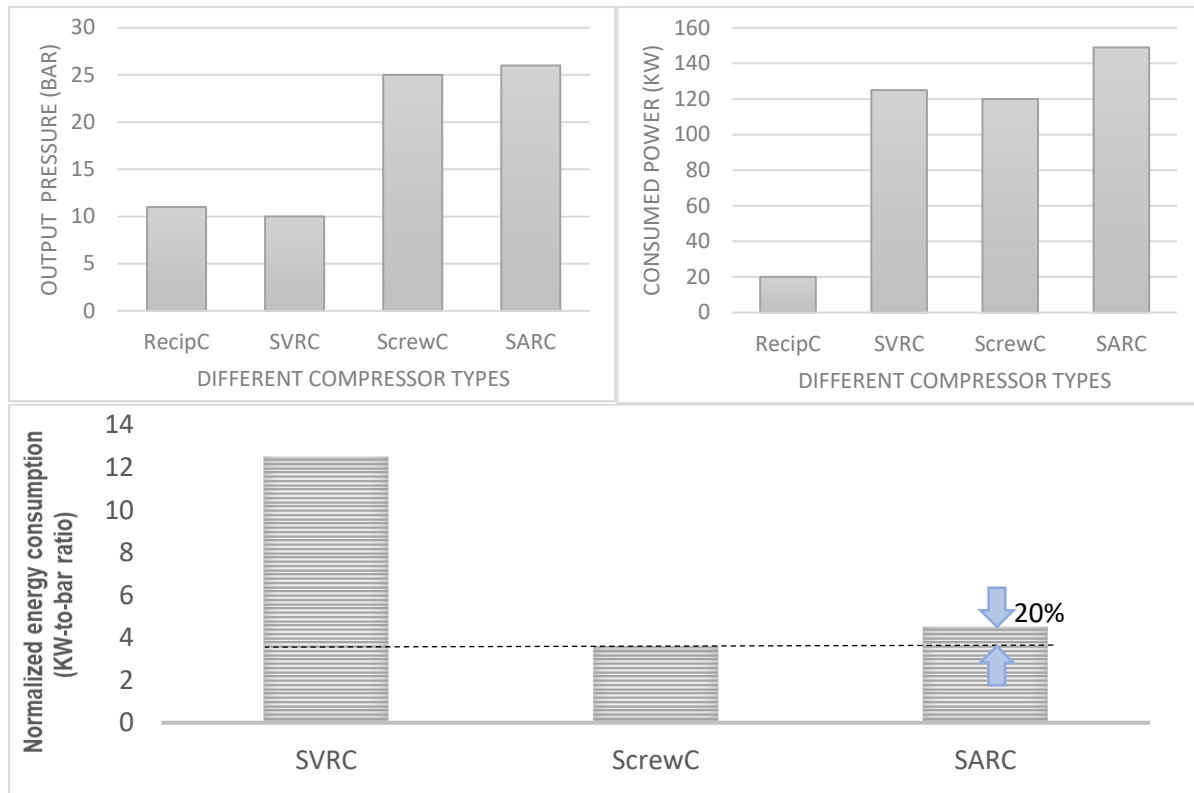


Figure 10 – Comparison of different types for big size applications

The small-size compressor has a 6-bar higher output pressure, and it needs 32% lower power compared to the best reciprocating compressor (**Figure 8**). The medium-size compressor has a 5-bar higher peak-pressure, and it needs 38% lower power (Figure 9). Finally, the big-size compressor has a 1-bar higher output pressure and 20% higher power consumption compared to the screw compressor, but its weight equals to the 39% of the screw compressor’s weight and its volume to the 26% of the screw compressor's volume.

Overall Weight and Volume comparison

The weight and volume of this type of compressor are calculated by using the full detailed 3D CAD model created in Solidworks. Afterwards, they are compared with the best competitors-compressors in the market for each application (Table 4).

Finally, this type of compressor needs no lubrication for its operation and cooling. Therefore, it is ideal for applications where the working medium should remain unmixed with any other material (Table 5).

Table 4 – Weight and Volume comparison

	<i>Small-size</i>	<i>Medium-size</i>	<i>Big-size</i>
<i>SARC weight (kg)</i>	26	86	393
<i>Lightest Compressor (kg)</i>	50 (↑ 96%)	180 (↑ 109%)	1000 (↑ 154%)
<i>Installation Volume for SARC (L)</i>	28	100	391
<i>Installation Volume for the smallest Compressor (L)</i>	200 (↑ 614%)	500 (↑ 400%)	1500 (↑ 284%)

Table 5 – Type of Lubricant in every compressor type

	<i>Reciprocating</i>	<i>SVRC</i>	<i>ScrewC</i>	<i>ScrollC</i>	<i>SARC</i>
<i>Lubricant</i>	Oil	Oil or Synthetic	Oil or Synthetic	Oil	No

7. CONCLUSIONS AND FUTURE WORK

The study is based on the real mechanical drawings of a compressor. Its construction will start the following month for conducting an experimental campaign.

The CFD models are based on the strict manufacturing constraints and real dimensions of the experimental device.

The under-study parameters for the three different size of compressors are:

- 1) the length of the sealing system, and
- 2) the intake-port configuration.

Depending on the size of the application, the conclusions of the analysis are the following:

1. The short sealing system's length is from 4% up to 9% more efficient than the long one
2. The optimised intake-port configuration increases the pressure output from 4% up to 6%
3. This technology can make an up to 27bar compression with a single stage compression process, while any other technology needs more than two compression stages to achieve this pressure
4. Its isentropic efficiency is from 54% up to 93%
5. This type of compressor can be up to 48% lighter and 86% smaller compared to its competitors for small-size applications
6. It can be up to 52% lighter and 80% smaller for medium-size applications
7. It can be up to 61% lighter and 74% smaller compared to its competitors for big-size applications
8. This kind of compressor can have an oil-free operation while most of its competitors, especially in high-pressure outputs need lubrication for cooling. The oil-free operation is very crucial especially for gases and mixtures sensitive to oil mixture because their properties can change with the oil mix. The oil-free operation is one of its most significant advantages because only a small amount (under 20%) [2] of all compressors could operate in oil-free conditions and with a pressure output up to 12 bar
9. This compressor is expected to have a low noise operation because there is no reciprocating motion or eccentric rotation of any of its components

The next step is to set up the experimental campaign and examines if the calculated results are confirmed.

ACKNOWLEDGEMENTS

We would like to warmly thank all companies that offered their software and technical support for free in order to conduct this research and help this compressor to uncover its benefits. More specifically, many thanks to:

- Dassault Systemes SolidWorks Corporation & the technical support from Innovera for helping us to create the 3D CAD model with SolidWorks,
- BETA CAE Systems & its technical support for helping us to prepare the model for the solver with ANSA
- CONVERGENT SCIENCE & its technical support for helping us to run our CFD simulations with their solver CONVERGE CFD
- BETA CAE Systems & its technical support for helping us to visualize the results from the solver with META

REFERENCES

- [1] P. Radgen, Compressed air systems in the European Union: energy, emissions, savings potential and policy actions., LOG_X Verlag GmbH, 2001.
 - [2] US Department of Energy and Energy Efficiency and Renewable Energy, Improving Compressed Air System Performance: a sourcebook for industry, US, 2003.
-

- [3] R. Cipollone und D. Vittorini, „Energy saving portential in existing compressors,“ *In Proceedings of the 22nd International Compressor Engineering Conference, Purdue University*, 2014.
- [4] H. P. Bloch, *A Particular Guide to Compressor Technology* by Heintz P. Bloch, 2006-09-14.
- [5] C. Antony Barber, „in Pneumatic Handbook (Eight Edition),“ in *Pneumatic Handbook*, 1997.
- [6] C. I. Ferreira, C. Zamfirescu und D. Zaytsev, „Twin Screw oil-free wet compressor for compression-absorbing cycle,“ *International Journal for Refrigeration*, pp. 29(4): 556 - 565, 2006.
- [7] „<http://www.remeza.com/en/catalog>,“ REMEZA, 2019. [Online].
- [8] R. Cipollone, G. Bianchi und G. Contaldi, „Sliding Vane Rotary Compressor energy optimization,“ *ASME 2012 International Mechanical Engineering Congress and Exposition, American Society of Mechanical Engineers*, pp. 69-80, 2012.
- [9] S. Savvakis. US Patent PCT/GR2006/000027, 2006.
- [10] G. Traskas und S. Savvakis, „Investigation of the sealing method for a new concept rotary engine,“ *7th before reality*, 2018.
- [11] N. Karakioulachis, S. Savvakis und Z. Samaras, „Sensitivity analysis of the dimensions and operating conditions of a new concept rotary engine,“ *7th before reality*, 2018.
- [12] „The SARM project: Operating Principle ans Model Desing,“ 2015. [Online]. Available: <http://www.thesarmproject.com>.
- [13] J. Heywood, *Internal Combustion Engine Fundamentals*, USA: McGraw Hill USA, 1988.
- [14] *Converge CFD 2.4 Manual*, CONVERGE CFD, 2018.
- [15] Thompson, Wowczuk und Smith, „Rotary Engines - A Concept Review,“ *SAE Technical Paper 2003-01-3206*, 2003.
- [16] J. Moran M., N. Shapiro H., D. Boettner und B. Bailey M., *Principle of Engineeering Thermodynamics*, Eight Edition, John Wiley & Sons, 2014.
- [17] V. Goutzamanis, S. Savvakis und A. Kalfas, „Numerical simulation of a novel rotary engine compared to conventional reciprocating engine cycle,“ *GPPS-2017-147*, 2017.
- [18] V. Goutzamanis, S. Savvakis und Z. Samaras , „Description of a Novel Concentric Rotary Engine,“ *2018-01-0365 SAE Technical Paper*, 2018.
- [19] BETA CAE SYSTEMS, *ANSA version 17.0.0 User's Guide*, Thessaloniki: BETA CAE SYSTEMS, July 2015.
- [20] J. D. Anderson, *Computational Fluid Dynamics, The Basics with Applications*, USA: McGrew Hill, 1995.
- [21] S. Savvakis, PhD: *Computational Investigation of a novel concentric rotary engine*, Thessaloniki: Aristotle University of Thessaloniki, 2011.

NOMENCLATURE

θ	angular coordinate (degrees)	\dot{m}	mass flow rate (kg/s)
F	force (N)	ρ	density (kg/m ³)
P	pressure (Pa)	V	velocity (m/s)
c_p	specific heat at const. p (J/kg/K)	W	Work (Joule)
T	temperature (K)	s	Entropy (J/K)
q	thermal power (W)	h	Enthalpy (Joule)
m	air or gas mass (kg)		
